Circulation
JOURNAL OF THE AMERICAN HEART ASSOCIATION

American Heart Association®
Learn and Live℠

Does Stringent Restrictive Annuloplasty for Functional Mitral Regurgitation Cause Functional Mitral Stenosis and Pulmonary Hypertension?

Satoshi Kainuma, Kazuhiro Taniguchi, Takashi Daimon, Taichi Sakaguchi, Toshihiro Funatsu, Haruhiko Kondoh, Shigeru Miyagawa, Koji Takeda, Yasuhiro Shudo, Takafumi Masai, Shinichi Fujita, Masami Nishino, Yoshiki Sawa and Osaka Cardiovascular Surgery Research (OSCAR) Group

Circulation 2011, 124:S97-S106
doi: 10.1161/CIRCULATIONAHA.110.013037
Circulation is published by the American Heart Association. 7272 Greenville Avenue, Dallas, TX 72514
 Print ISSN: 0009-7322. Online ISSN: 1524-4539

Does Stringent Restrictive Annuloplasty for Functional Mitral Regurgitation Cause Functional Mitral Stenosis and Pulmonary Hypertension?

Satoshi Kainuma, MD; Kazuhiro Taniguchi, MD, PhD; Takashi Daimon, PhD; Taichi Sakaguchi, MD, PhD; Toshihiro Funatsu, MD, PhD; Haruhiko Kondoh, MD, PhD; Shigeru Miyagawa, MD, PhD; Koji Takeda, MD, PhD; Yasuhiro Shudo, MD; Takafumi Masai, MD, PhD; Shinichi Fujita, CE; Masami Nishino, MD, PhD; Yoshiki Sawa, MD, PhD; Osaka Cardiovascular Surgery Research (OSCAR) Group

Background—It remains controversial whether restrictive mitral annuloplasty (RMA) for functional mitral regurgitation (MR) can induce functional mitral stenosis (MS) that may cause postoperative residual pulmonary hypertension (PH).

Methods and Results—One hundred eight patients with left ventricular (LV) dysfunction and severe MR underwent RMA with stringent downsizing of the mitral annulus. Systolic pulmonary artery pressure (PAP) and mitral valve performance variables were determined by Doppler echocardiography prospectively and 1 month after RMA. Fifty-eight patients underwent postoperative hemodynamic measurements. Postoperative echocardiography showed a mean pressure half-time of 92±14 ms, a transmitral mean gradient of 2.9±1.1 mm Hg, and a mitral valve effective orifice area of 2.4±0.4 cm^2, consistent with functional MS. Doppler-derived systolic PAP was 32±8 mm Hg, which correlated weakly with the transmitral mean gradient (ρ=0.23, P=0.02). Postoperative cardiac catheterization also showed significant improvements in LV volume and systolic function, pulmonary capillary wedge pressure, cardiac index, and systolic PAP; the latter was associated with LV end-diastolic pressure [standardized partial regression coefficient (SPRC)=0.51], pulmonary vascular resistance (SPRC=0.47), cardiac index (SPRC=0.37), and transmitral pressure gradient (SPRC=0.20). In a multivariate Cox proportional hazard model, postoperative PH (systolic PAP >40 mm Hg), but not mitral valve performance variables, was strongly associated with adverse cardiac events.

Conclusions—RMA for functional MR resulted in varying degrees of functional MS. However, our data were more consistent with the residual PH being caused by LV dysfunction and pulmonary vascular disease than by the functional MS. The residual PH, not functional MS, was the major predictor of post-RMA adverse cardiac events. **(*Circulation*. 2011;124[suppl 1]:S97–S106.)**

Key Words: functional mitral regurgitation ■ cardiomyopathy ■ restrictive mitral annuloplasty ■ functional mitral stenosis ■ pulmonary hypertension ■ patient-prosthesis mismatch

Restrictive mitral annuloplasty (RMA), which involves the insertion of an undersized prosthetic ring, has become the preferred surgical option for the treatment of patients with medically uncontrollable, severe functional mitral regurgitation (MR). Previous studies[1–4] have shown that stringent RMA can effectively eliminate functional MR, resulting in reverse left ventricular (LV) remodeling, and improved symptoms, and survival in the great majority of patients.

In contrast to these beneficial effects of the RMA procedure, Magne et al[5] first reported that the insertion of such an undersized ring may induce an iatrogenic "functional" mitral stenosis (MS) similar to prosthesis-patient mismatch (PPM), a condition that is frequently found after mitral valve replacement with a small prosthetic valve.[6–8] The effective orifice area (EOA) of a prosthetic valve or annuloplasty ring is often too small in relation to body size, causing a mismatch between the EOA and the transmitral flow, and yielding relatively high gradients. Several recent studies have reported a high incidence of functional MS, in which the mitral valve area is less than 1.5 cm^2[9] or the mean pressure gradient is greater than 5 mm Hg, after RMA.[10] In contrast, most prior

From the Department of Cardiovascular Surgery (S.K., Ka.T., T.F., H.K.), Division of Cardiology (M.N.), and Clinical Echocardiography Section (S.F.), Japan Labor Health and Welfare Organization Osaka Rosai Hospital, Sakai, Osaka, Japan; the Department of Cardiovascular Surgery (S.K., T.S., S.M., Ko.T., Ya.S., Yo.S.), Osaka University Graduate School of Medicine, Suita, Osaka, Japan; the Department of Cardiovascular Surgery (T.M.), Sakurabashi Watanabe Hospital, Osaka, Japan; and the Department of Biostatistics (T.D.), Hyogo College of Medicine, Nishinomiya, Hyogo, Japan.

Presented at the 2010 American Heart Association meeting in Chicago, IL, November 12–16, 2010.

Correspondence to Yoshiki Sawa, MD, Department of Cardiovascular Surgery, Osaka University Graduate School of Medicine, Suita, Osaka 565-0871, Japan. E-mail Sawa@surg1.med.osaka-u.ac.jp

Circulation **is available at http://circ.ahajournals.org** **DOI: 10.1161/CIRCULATIONAHA.110.013037**

echocardiographic studies did not describe problems with functional MS or ring PPM after mitral valve repair using an undersized annuloplasty ring.[3,4]

Magne et al[5] also found that this hemodynamic consequence (functional MS) may be associated with residual pulmonary hypertension (PH) after RMA. However, little data from invasive hemodynamic monitoring techniques with regard to functional MS have been reported. The purpose of this study was to evaluate the post-RMA hemodynamic data, to determine whether stringent RMA for functional MR results in functional MS, and whether this hemodynamic consequence is mainly responsible for residual PH after the operation. We also attempted to determine factors predicting residual PH and short-term outcome in patients undergoing the RMA procedure.

Methods

Patients

Between July 2003 and November 2009, 195 patients underwent RMA for functional MR using a semirigid complete ring (Carpentier-Edwards Physio ring; Edwards Lifesciences, Irvine, CA) at 3 university-affiliated hospitals. Functional MR associated with cardiomyopathy was defined as a combination of moderate-to-severe MR with (1) a history of at least 1 hospitalization for heart failure in the previous 6 months, despite maximal medical treatment, (2) global LV dysfunction (LV ejection fraction <40%) with a significantly enlarged left ventricle, and (3) type IIIb leaflet dysfunction, according to Carpentier classification. Of these patients, 87 were excluded because of concomitant surgical ventricular reconstruction (n=69), redo mitral valve surgery owing to MR recurrence (n=4), postoperative infective endocarditis (n=2), or early hospital death (n=12). The final study population consisted of 108 patients (86 men, 22 women), who had a mean body surface area (BSA) of 1.65±0.19 cm^2 (range, 1.30 to 2.26). Because the patients with a 26-mm Physio ring had a larger BSA than those with a 24-mm Physio ring, patient baseline characteristics are presented according to the size of the ring (Table 1). Before surgical referral, all the patients had been treated with optimized medical regimens by his or her attending cardiologist, including angiotensin-converting enzyme inhibitors or angiotensin-receptor blockers, β-blockers, and diuretics.

Ethical committee approval was obtained from each institution, and individual consent was waived for this retrospective analysis. Written informed consent for the procedure was obtained from each patient before surgery.

Echocardiography

Two-dimensional and Doppler transthoracic echocardiography examinations were performed before and 1 month after surgery. All echocardiographic studies were done using commercially available 3.75-MHz transducers (Toshiba, Tokyo, Japan, and Hewlett-Packard Sonos) by expert echocardiographic examiners who were blinded to the clinical status of the patients and their operative data. Echocardiographic measurements included LV end-diastolic and end-systolic dimensions, LA dimension, LV ejection fraction, and right ventricular (RV) end-diastolic dimension. Postoperative transmitral mean gradient were measured by Doppler echocardiography. The mitral valve EOA was determined by the pressure half-time method[11] and indexed for BSA. The severity of regurgitation was classified as none (0), trivial (1+), mild (2+), moderate (3+), or severe (4+) in the present study.

Doppler-Derived Pulmonary Artery Pressure

Systolic pulmonary artery pressure (PAP) was calculated by adding the systolic pressure gradient across the tricuspid valve derived from tricuspid regurgitation, to the estimated right atrial pressure value.[12,13]

Table 1. Patient Characteristics

Variables	Physio 24 mm (n=66)	Physio 26 mm (n=42)
Age, y	67±9	63±9
Males	47 (71%)	39 (93%)
Body surface area, m^2	1.61±0.19	1.70±0.17*
New York Heart Association class		
I	0 (0%)	0 (0%)
II	2 (3%)	3 (7%)
III	54 (81%)	24 (57%)
IV	10 (15%)	15 (36%)
Echocardiographic data		
LV end-diastolic dimension, mm	64±6	70±9*
LV end-systolic dimension, mm	54±7	60±11*
LV ejection fraction, %	29±8	29±8
Left atrial dimension, mm	46±7	50±9
RV end-diastolic dimension, mm	33±7	33±5
Systolic PAP, mm Hg	46±14	47±13
Mitral regurgitation, 0/1+/2+/3+/4+	0/0/0/38/28	0/0/0/17/25
Tricuspid regurgitation, 0/1+/2+/3+/4+	2/22/17/16/9	2/7/21/11/1
ECG		
Left bundle-branch block	14 (21%)	9 (21%)
QRS duration >130 ms	13 (20%)	11 (26%)
History of cardiac resynchronization therapy	2 (3%)	5 (12%)
DDD pacemaker	1 (2%)	0 (0%)
Comorbidity		
Hypertension	39 (59%)	19 (45%)
Diabetes	36 (55%)	17 (40%)
Hyperlipidemia	28 (42%)	12 (29%)
Chronic obstructive lung disease	4 (6%)	4 (10%)
Chronic renal failure	27 (41%)	16 (38%)
Peripheral vascular disease	10 (15%)	3 (7%)
Cerebral vascular accident	14 (21%)	6 (14%)
Atrial fibrillation	24 (36%)	14 (33%)
History of ventricular arrhythmia	7 (11%)	12 (29%)
Previous cardiac surgery	6 (9%)	1 (2%)
Etiology of cardiomyopathy		
Idiopathic	22 (33%)	20 (48%)
Ischemic	44 (67%)	22 (52%)
Medications		
β-Blockers	43 (65%)	24 (57%)
ACE inhibitors	17 (26%)	6 (14%)
Angiotensin II receptor blockers	25 (38%)	8 (19%)
Long-acting nitrates	11 (17%)	8 (19%)
Diuretics	48 (73%)	26 (62%)
Operative data		
Cardiopulmonary bypass time, min	181±62	189±63
Aortic cross-clamp time, min	97±44	110±45
Concomitant procedures		
Coronary artery bypass grafting	27 (41%)	19 (45%)
Tricuspid annuloplasty	47 (71%)	21 (50%)
Modified maze procedure	16 (24%)	13 (31%)
Pulmonary vein isolation	8 (12%)	1 (2%)

LV indicates left ventricular; RV, right ventricular; PAP, pulmonary artery pressure; ACE, angiotensin converting enzyme; and NS, not significant ($P>0.05$).

*$P<0.05$ versus Physio 24-mm.

Cardiac Catheterization

Right and left heart catheterization procedures were performed, using standard techniques before and 1 month (within 1 day of echocardiography) after surgery. The purposes of the cardiac catheterization and the invasive nature of the procedure were explained in detail to all patients, and only those who gave informed consent underwent catheterizations. The indications for postoperative catheterization were not selective. None had complications at the preoperative or postoperative catheterization. As a result, preoperative coronary arteriography was performed for all 108 patients, but left ventriculography and hemodynamic measurements were performed for 97 (90%) and 75 (69%), respectively. After surgery, 89 of the 108 patients (82%) underwent left ventriculography and 58 (54%) underwent hemodynamic measurements.

Before left ventriculography, standard pressure measurements were obtained to evaluate the LV systolic pressure, LV end-diastolic pressure (LVEDP), pulmonary capillary wedge pressure (PCWP); systolic, diastolic, and mean PAP; RV systolic pressure, RVEDP, and right atrial pressure. Right-sided pressures were obtained using a Swan-Ganz catheter. Cardiac output was determined with the thermodilution method. In addition, the systemic vascular resistance (SVR) and pulmonary vascular resistance (PVR) were also calculated.

Hemodynamic Assessment of Mitral Valve Performance

The gradient across the mitral valve was calculated as the pressure difference between mean PCWP and LVEDP, although it is better to determine transmitral gradients using simultaneous recordings.

Classification of the Severity of MS, Prosthesis-Patient Mismatch, and PH

MS severity was categorized classically as mild (EOA >1.5 cm^2, mean gradient <5 mm Hg), moderate (EOA 1.0 to 1.5 cm^2, mean gradient 5 to 10 mm Hg), or severe (EOA <1.0 cm^2, mean gradient >10 mm Hg).

Indeed, there is no single parameter that defines the severity of functional MS that is possibly induced by an RMA procedure. In the present study, functional MS severity was categorized according to the level of the in vivo EOA in relation to patient body size; PPM was defined as mild and not clinically significant if the indexed EOA was >1.2 cm^2/m^2, as moderate if it was >0.9 to 1.2 cm^2/m^2, and as severe if it was ≤ 0.9 cm^2/m^2.[8]

The severity of PH was also categorized as mild (systolic PAP <40 mm Hg), moderate (systolic PAP 40 to 60 mm Hg), or severe (systolic PAP >60 mm Hg).

Surgical Procedures

A median sternotomy was performed under a mild hypothermic cardiopulmonary bypass with intermittent cold blood cardioplegia. A stringent restrictive (2 to 3 sizes smaller than measured) mitral annuloplasty was performed for all patients. The ring size was selected according to the surgeon's preference (Ka.T., T. M., and Y.S.) at each hospital, considering the patient's body size. Sixty-six (61%) patients received a 24-mm Physio ring (geometric orifice area, 2.74 cm^2) and 42 (39%) a 26-mm Physio ring (geometric orifice area, 3.25 cm^2). Data regarding the geometric orifice area of the ring were supplied by the manufacturer. All relevant surgical data are summarized in Table 1.

Clinical Follow-Up

Clinical follow-up examinations were completed for all 108 patients (100%), with a mean duration of 33 ± 18 months. Every 6 months to 1 year, each patient was assessed in the department as well as by his or her primary cardiologist. A retrospective review of the medical records of these patients was performed to obtain the preoperative and postoperative data. Current information was obtained by calling the patient or the referring cardiologist. We also reviewed the postoperative adverse cardiac events defined as late cardiac-related death, myocardial infarction, thromboembolism, readmission for heart failure, and ventricular arrhythmia requiring implantation of an intracardiac defibrillator.

Statistical Analysis

Continuous variables are summarized as mean$\pm$SD and categorical variables as frequencies and proportions. All the continuous variables were checked for normality using the Shapiro-Wilk test and normal probability plot. Normally distributed variables were compared using the Student t test and nonnormally distributed variables were compared with the Mann-Whitney U test. Categorical variables were compared using the χ^2 analysis or Fisher exact test, as appropriate. Preoperative and postoperative hemodynamic variables were assessed by repeated-measures ANOVA with group, time, and group-time interaction effects. Nonnormally distributed variables tested in the repeated ANOVA were natural log-transformed to satisfy normality of the used models, as appropriate. Correlation between nonnormally distributed variables were tested with Spearman correlation coefficient (ρ).

Stepwise multiple linear regression analyses were performed to identify the determinants of Doppler-derived or catheter-measured systolic PAP. The Doppler-derived systolic PAP and catheter-measured systolic PAP were natural log-transformed to satisfy normality of the used models. Factors obtaining a probability value less than 0.1 in the univariate analysis, based on Spearman correlation coefficient were then entered appropriately into the stepwise multiple linear regression model. Regression diagnostics was used to assess the obtained models for collinearity and residual nonnormality and heteroscedasticity. The results are summarized as correlation coefficients (ρ) and standardized partial regression coefficients (SPRCs).

Univariate and multivariate analyses of the predictors for adverse cardiac time to events were performed using Cox proportional hazards models. Factors obtaining a probability value less than 0.1 in the univariate Cox proportional hazards analysis were then entered appropriately into the multivariate fashion, using stepwise variable selection. The results are summarized as hazard ratios (HRs) and 95% confidence intervals (CIs). Statistical significance was defined as a probability value <0.05. Statistical analyses were performed using JMP 7.0 (SAS Institute, Cary, NC) and SPSS software (version 17.0, SPSS Inc).

Results

Postoperative Echocardiographic Data

After surgery, none of the patients showed a significant ($>2+$) level of residual MR (Table 2). The pressure half-time was 92 ± 14 ms in all the patients (range, 67 to 129 ms versus normal value, 40 to 60 ms), which was prolonged and suggested the presence of gradients across the mitral valve. The transmitral mean gradient value was 2.9 ± 1.1 mm Hg (range, 1.1 to 6.2 mm Hg). Ninety-eight of the 108 patients (91%; 95% CI, 84% to 95%) had a transmitral mean gradient value <5 mm Hg (mild MS), whereas 10 (9%; 95% CI, 5% to 16%) had a mean gradient value ≥ 5 mm Hg (moderate MS). The mitral valve EOA value was 2.4 ± 0.4 cm^2 (range, 1.7 to 3.3 cm^2), and none of the patients had a value <1.5 cm^2. The indexed EOA value was 1.51 ± 0.32 cm^2/m^2 (range, 0.84 to 2.46 cm^2/m^2). Twenty-one (19%; 95% CI, 13% to 28%) showed moderate PPM (an indexed EOA >0.9 to ≤ 1.2 cm^2/m^2), and 2 (2%; 95% CI, 0.5 to 6.5%) had severe PPM (an indexed EOA ≤ 0.9 cm^2/m^2). The mean value for systolic PAP was 32 ± 8 mm Hg (range, 18 to 53 mm Hg). Seventeen patients (16%; 95% CI, 11% to 26%) showed moderate PH (systolic PAP, 40 to 60 mm Hg), and none had severe PH (systolic PAP >60 mm Hg) after surgery. Notably, patients with a 24-mm ring

Table 2. Postoperative Echocardiographic Measurements

Variables	All Cases (n=108)	Physio 24 mm (n=66)	Physio 26 mm (n=42)	*P* Value*
Geometric orifice area, cm^2		2.74	3.25	
Indexed GOA, cm^2/m^2	1.80±0.22	1.72±0.20	1.93±0.19	<0.001
Pressure half-time, ms	92±14	96±15	86±11	<0.001
Mitral mean gradient, mm Hg	2.9±1.1	3.1±1.1	2.6±1.1	0.01
<5 mm Hg	98 (91%)	58 (88%)	40 (95%)	NS
≥5 mm Hg	10 (9%)	8 (12%)	2 (5%)	
Mitral valve EOA, cm^2	2.4±0.4	2.3±0.4	2.6±0.3	<0.001
≥1.5 cm^2	108 (100%)	66 (100%)	42 (100%)	NS
<1.5 cm^2	0 (0%)	0 (0%)	0 (0%)	
Mitral valve EOA/GOA	0.83±0.12	0.86±0.13	0.80±0.10	0.01
Indexed EOA, cm^2/m^2	1.51±0.32	1.48±0.34	1.54±0.27	NS
>1.2 cm^2/m^2	85 (79%)	48 (73%)	37 (88%)	NS
>0.9 to 1.2 cm^2/m^2	21 (19%)	17 (26%)	4 (10%)	
≤0.9 cm^2/m^2	2 (2%)	1 (1%)	1 (2%)	
Indexed EOA/GOA, $/m^2$	0.52±0.11	0.54±0.12	0.48±0.08	0.003
Systolic PAP, mm Hg	32±8	31±9‡	32±6‡	NS
Not determined†	9 (8%)	5 (8%)	4 (10%)	NS
<40 mm Hg	82 (76%)	51 (77%)	31 (74%)	
40–60 mm Hg	17 (16%)	10 (15%)	7 (17%)	
>60 mm Hg	0 (0%)	0 (0%)	0 (0%)	
LV end-diastolic dimension, mm	61±9	59±7‡	64±10‡	NS
LV end-systolic dimension, mm	52±11	50±9‡	55±12‡	0.04
LV ejection fraction, %	33±10	34±10‡	32±10‡	NS
Left atrial dimension, mm	43±7	42±6‡	45±8‡	NS
RV end-diastolic dimension, mm	29±6	30±6‡	27±6‡	NS
Residual mitral regurgitation, 0/1+/2+/3+/4+	66/34/8/0/0	40/22/4/0/0	26/12/4/0/0	NS
Residual tricuspid regurgitation, 0/1+/2+/3+/4+	9/86/13/0/0	5/56/5/0/0	4/30/8/0/0	NS

GOA indicates geometric orifice area; EOA, effective orifice area; PAP, pulmonary artery pressure; LV, left ventricular; and RV, right ventricular.

*Physio 24-mm versus Physio 26-mm.

†Data were not available due to absence of tricuspid regurgitation.

‡$P<0.05$ versus variables at baseline in each group.

had a greater mean transmitral gradient, smaller mitral valve EOA, and longer pressure half-time compared with those with a 26-mm ring, whereas there was no difference between the groups with regard to the indexed EOA and systolic PAP. In general, the transmitral mean gradient correlated inversely with the indexed EOA value ($\rho=-0.30$ $P=0.002$), and correlated positively with the BSA ($\rho=0.27$, $P=0.006$).

Other LV dimension and function variables substantially improved in both groups.

Determinants of Postoperative Doppler-Derived Systolic PAP 1 Month After RMA

Postoperative Doppler-derived systolic PAP correlated with the Doppler-derived transmitral mean gradient ($\rho=0.23$, $P=0.02$) but did not correlate with the EOA or indexed EOA(Table 3). Postoperative systolic PAP also correlated with the catheter-derived postoperative PCWP ($\rho=0.40$, $P=0.002$), LVEDP ($\rho=0.38$, $P=0.004$), and PVR ($\rho=0.66$, $P<0.001$). Multivariate analysis showed that PVR had the most important contribution (SPRC=0.62), followed by LVEDP (SPRC=0.28), whereas the transmitral gradient had a minimal contribution (SPRC=0.24). Postoperative PCWP was not entered into the multivariate analysis because of a strong correlation between PCWP and LVEDP ($\rho=0.87$). Regression diagnostics showed no evidence of collinearity and residual nonnormality and heteroscedasticity in the obtained models.

Preoperative and Postoperative Hemodynamic Data

From baseline to 1 month after surgery, LV volumes decreased and ejection fraction improved in both patient groups (Table 4). LV systolic pressure did not change, whereas LVEDP, PCWP, systolic, and mean PAP decreased significantly. Other hemodynamic parameters such as cardiac index, PVR, and SVR also improved significantly or showed a trend toward normal in both groups. Importantly, there were no differences in postoperative LV function or hemodynamic parameters between the 2 groups, which received different sized rings.

Table 3. Determinants of Postoperative Doppler-Derived Systolic PAP 1 Month After RMA

	Univariate		Multivariate	
Variables	ρ	*P* Value	SPRC	*P* Value
Preop echocardiographic parameters (n=108)				
LVEDD, mm		NS		
LVESD, mm		NS		
LV ejection fraction, %		NS		
LA dimension, mm	0.22	0.03		
RVEDD, mm		NS		
Systolic PAP, mm Hg	0.35	<0.001		
Preop volume and function parameters (n=97)				
LVEDVI, mL/m^2		NS		
LVESVI, mL/m^2		NS		
LV ejection fraction, %		NS		
Preop hemodynamic parameters (n=75)				
LVSP, mm Hg		NS		
LVEDP, mm Hg	0.21	0.08		
PCWP, mm Hg	0.21	0.08		
Systolic PAP, mm Hg	0.21	0.08		
Cardiac index, L/min/m^2	−0.28	0.009		
PVR, dyne · s · cm^{-5}	0.63	<0.001		
SVR, dyne · s · cm^{-5}	0.26	0.02		
Postop echocardiographic parameters (n=108)				
LVEDD, mm		NS		
LVESD, mm		NS		
LV ejection fraction, %		NS		
LA dimension, mm	0.18	0.07		
RVEDD, mm		NS		
Mitral valve EOA, cm^2		NS		
Indexed EOA, cm^2/m^2		NS		
Pressure half-time, ms		NS		
Mitral mean gradient, mm Hg	0.23	0.02	0.24	0.01
Postop volume and function parameters (n=89)				
LVEDVI, mL/m^2		NS		
LVESVI, mL/m^2	0.25	0.02		
LV ejection fraction, %	−0.26	0.02		
Postop hemodynamic parameters (n=58)*				
LVSP, mm Hg		NS		
LVEDP, mm Hg	0.38	0.004	0.28	0.01
PCWP, mm Hg†	0.40	0.002		
Mitral gradient (mean PCWP-LVEDP), mm Hg		NS		
Cardiac index, L/min/m^2		NS		
PVR, dyne · s · cm^{-5}	0.66	<0.001	0.62	<0.001
SVR, dyne · s · cm^{-5}		NS		

SPRC indicates standardized partial regression coefficient; LV, left ventricular; RV, right ventricular; PAP, pulmonary artery pressure; PCWP, pulmonary capillary wedge pressure; PVR, pulmonary vascular resistance; SVR, systemic vascular resistance; EOA, effective orifice area; LVEDD, left ventricular end-diastolic dimension; LVESD, left ventricular end-systolic dimension; LA, left atrial; RVEDD, right ventricular end-diastolic dimension; LVEDVI, left ventricular end-diastolic volume index; LVESVI, left ventricular end-systolic volume index; LVSP, left ventricular systolic pressure; and NS, not significant ($P>0.05$).

*Postoperative catheter-measured systolic PAP was not tested in this analysis.

†Postoperative PCWP was not entered into the multivariate analysis because of a strong correlation between PCWP and LVEDP ($\rho=0.87$).

The postoperative transmitral pressure gradient value, calculated as the pressure difference between mean PCWP and LVEDP, was 3.0±1.2 mm Hg (range, 1 to 7 mm Hg). The mean value for catheter-measured postoperative systolic PAP was 33±8 mm Hg (range, 18 to 54 mm Hg). Fifteen of the 58 patients (26%; 95% CI, 16% to 38%) showed moderate PH (systolic PAP, 40 to 60 mm Hg), and none had severe PH (systolic PAP, >60 mm Hg) after surgery. Notably, patients with a 24-mm ring had greater transmitral pressure gradients compared with patients with a 26-mm ring, whereas there was no difference in systolic PAP between the groups. There were also no differences for the other hemodynamic measurements.

In general, the transmitral pressure gradient correlated positively with cardiac output ($\rho=0.77$, $P<0.001$) and heart rate ($\rho=0.27$, $P=0.05$).

Determinants of Postoperative Catheter-Measured Systolic PAP 1 Month After RMA

In univariate analyses, the postoperative catheter-measured systolic PAP correlated with the PCWP ($\rho=0.70$, $P<0.001$), LVEDP ($\rho=0.56$, $P<0.001$), transmitral pressure gradient ($\rho=0.52$, $P<0.001$), cardiac index ($\rho=0.28$, $P=0.04$), and PVR ($\rho=0.54$, $P<0.001$) (Table 5). Multivariate analysis showed that LVEDP had the most important contribution (SPRC=0.51), followed by PVR (SPRC=0.47) and the cardiac index (SPRC=0.37), whereas the transmitral pressure gradient had a minimal contribution (SPRC=0.20). Postoperative PCWP was not entered into the multivariate analysis because of a strong correlation between PCWP and LVEDP ($\rho=0.87$). Regression diagnostics showed no evidence of collinearity, and residual nonnormality and heteroscedasticity in the obtained models.

Correlation Between Invasive Hemodynamic Measurements and Noninvasive Doppler-Derived Variables

Spearman correlation analysis showed a strong correlation ($\rho=0.94$, $P<0.001$) between the catheter-measured mitral pressure gradient and Doppler-derived transmitral mean gradient values. There was also a substantial correlation

Table 4. Preoperative and Postoperative Hemodynamic Measurements

	Physio No. 24 (n=32)		Physio No. 26 (n=26)				
Variables	Preop	Postop	Preop	Postop	Group	Time	Group-Time
LV end-diastolic volume index, mL/m^2	135±35	109±35	150±47	126±49	NS	<0.001	NS
LV end-systolic volume index, mL/m^2	101±30	78±33	113±44	90±48	NS	<0.001	NS
LV ejection fraction, %	26±7	30±12	26±8	31±12	NS	0.002	NS
LV systolic pressure, mm Hg	115±21	121±14	123±21	124±24	NS	NS	NS
LVEDP, mm Hg	17±6	9±3	17±7	11±3	NS	<0.001	NS
PCWP, mm Hg	21±6	13±3	21±8	13±3	NS	<0.001	NS
Mitral gradient (=mean PCWP−LVEDP), mm Hg		3.3±1.4		2.6±1.0*			
Systolic PAP, mm Hg	46±13	34±9	46±16	34±9	NS	<0.001	NS
<40 mm Hg	10 (31%)	24 (75%)	11 (42%)	19 (73%)			
40–60 mm Hg	19 (60%)	8 (25%)	10 (38%)	7 (27%)			
>60 mm Hg	3 (9%)	0 (0%)	5 (19%)	0 (0%)			
Mean PAP, mm Hg	32±7	21±6	33±9	22±6	NS	<0.001	NS
Right atrial pressure, mm Hg	8±4	8±3	7±4	8±2	NS	NS	NS
Heart rate, beats/min	78±11	79±13	76±15	81±10	NS	NS	NS
Cardiac index, L/min/m^2	2.7±0.7	2.9±0.7	2.3±0.6	2.8±0.6	NS	<0.001	0.02
Stroke volume index, mL/m^2	36±11	38±10	31±9	35±5	NS	0.02	NS
PVR, dyne · s · cm^{-5}	235±73	150±75	250±71	156±67	NS	<0.001	NS
SVR, dyne · s · cm^{-5}	1470±460	1370±440	1620±400	1220±250	NS	<0.001	0.02

LV indicates left ventricular; RV, right ventricular; PAP, pulmonary artery pressure; EDP, end-diastolic pressure; PCWP, pulmonary capillary wedge pressure; PVR, pulmonary vascular resistance; SVR, systemic vascular resistance; EOA, effective orifice area; and NS, not significant ($P>0.05$).

*$P<0.05$ versus Physio 24-mm.

($\rho=0.67$, $P<0.001$) between the catheter-measured systolic PAP and Doppler-derived systolic PAP values.

Clinical Outcomes

In this series, the actuarial survival rates at 1, 2, and 3 years after surgery were 95±2%, 92±3%, and 87±4%, respectively. During the follow-up period, there were 6 late cardiac-related deaths, 29 late readmissions due to heart failure, 1 myocardial infarction, and 4 ventricular arrhythmias. Freedom from adverse cardiac events at 1, 2, and 3 years after surgery was 88±3%, 78±4%, and 68±5%, respectively. There was no difference in freedom from adverse cardiac events between patients with an indexed EOA of >1.2 cm^2/m^2 versus ≤1.2 cm^2/m^2.

Among the preoperative variables investigated, preoperative PAP >60 mm Hg (HR, 4.5; 95% CI, 2.2 to 8.9) and a history of ventricular arrhythmia (HR 2.1, 95% CI: 1.0 to 4.6) were the predictors of the postoperative adverse cardiac events (Table 6). Furthermore, among the postoperative echocardiographic variables and surgical data, a postoperative PAP >40 mm Hg (HR, 4.6; 95% CI, 2.3 to 9.3) and residual tricuspid regurgitation (HR, 2.5; 95% CI, 1.0 to 6.1) were the predictors of adverse cardiac events (Table 7).

Discussion

This study constitutes an initial report evaluating the association between iatrogenic functional MS, PPM in terms of in vivo indexed EOA, residual PH, and clinical outcome (late adverse cardiac events) after RMA in patients with advanced cardiomyopathy.

The present echocardiographic results are largely consistent with those presented in previous studies, especially in terms of the transmitral mean gradient, mitral valve area, and systolic PAP.[3,4,14–16] In contrast, Magne et al[5] reported a higher mean gradient (6±2 mm Hg), smaller mitral valve area (1.5±0.3 cm^2), and higher systolic PAP (42±13 mm Hg) values compared with other prior studies. Among the 24 patients in their study, 54% (n=13) had a mean gradient ≥5 mm Hg, 54% (n=13) had a valve area ≤1.5 cm^2, and 45% (n=11) had a systolic PAP ≥40 mm Hg. From those findings, they concluded that a large proportion (>50%) of the patients who underwent RMA had moderate functional MS and significant PH after the operation. In addition, a recent study[9] also reported a high prevalence (42%) of patients with a small valve area, ≤1.5 cm^2. However, in that study, the transmitral gradients were similar to those reported in many other studies.[3,4,14–16]

In the present study, only 9% of the patients showed a mean gradient ≥5 mm Hg, and none had a valve area ≤1.5 cm^2. The contrasting results with regard to valve area as compared to the study of Magne et al[5] can be explained by the different methods utilized for determining valve area. Magne et al[5] calculated mitral valve area using the continuity equation, whereas many other investigators, including our group, determined it using the pressure half-time method or direct planimetry.[3,4,14–16] In addition, the difference in results for the transmitral gradient may be due to subject selection bias or the patient's BSA. The mean BSA of their patients was greater than that of our patients (1.8±0.2 m^2 versus 1.65±0.19 m^2). Magne et al[5] also found a significant corre-

Table 5. Determinants of Postoperative Catheter-Measured Systolic PAP 1 Month After RMA

	Univariate		Multivariate	
Variables	ρ	P Value	SPRC	P Value
Preop echocardiographic parameters (n=108)				
LVEDD, mm		NS		
LVESD, mm		NS		
LV ejection fraction, %		NS		
LA dimension, mm	0.35	0.007	0.23	0.009
RVEDD, mm		NS		
Systolic PAP, mm Hg	0.54	<0.001		
Preop volume and function parameters (n=97)				
LVEDVI, mL/m^2		NS		
LVESVI, mL/m^2		NS		
LV ejection fraction, %		NS		
Preop hemodynamic parameters (n=75)				
LVSP, mm Hg		NS		
LVEDP, mm Hg	0.26	0.08		
PCWP, mm Hg	0.28	0.06		
Systolic PAP, mm Hg	0.33	0.02		
Cardiac index, L/min/m^2		NS		
PVR, dyne · s · cm^{-5}	0.28	0.04		
SVR, dyne · s · cm^{-5}		NS		
Postop echocardiographic parameters (n=108)*				
LVEDD, mm		NS		
LVESD, mm		NS		
LV ejection fraction, %		NS		
LA dimension, mm	0.42	0.001		
RVEDD, mm		NS		
Mitral valve EOA, cm^2		NS		
Indexed EOA, cm^2/m^2		NS		
Pressure half-time, ms		NS		
Mitral mean gradient, mm Hg	0.52	<0.001	0.20	0.006
Postop volume and function parameters (n=89)				
LVEDVI, mL/m^2		NS		
LVESVI, mL/m^2		NS		
LV ejection fraction, %		NS		
Postop hemodynamic parameters (n=58)				
LVSP, mm Hg		NS		
LVEDP, mm Hg	0.56	<0.001	0.51	<0.001
PCWP, mm Hg†	0.70	<0.001		
Mitral gradient (mean PCWP−LVEDP), mm Hg	0.44	<0.001		
Cardiac index, L/min/m^2	0.28	0.04	0.37	<0.001
PVR, dyne · s · cm^{-5}	0.54	<0.001	0.47	<0.001
SVR, dyne · s · cm^{-5}		NS		

LV indicates left ventricular; RV, right ventricular; PAP, pulmonary artery pressure; PCWP, pulmonary capillary wedge pressure; PVR, pulmonary vascular resistance; SVR, systemic vascular resistance; EOA, effective orifice area; LVEDD, left ventricular end-diastolic dimension; LVESD, left ventricular end-systolic dimension; LA, left atrial; RVEDD, right ventricular end-diastolic dimension; LVEDVI, left ventricular end-diastolic volume index; LVESVI, left ventricular end-systolic volume index; LVSP, left ventricular systolic pressure; and NS, not significant ($P>0.05$).

*Postoperative Doppler-derived systolic PAP was not tested in this analysis.

†Postoperative PCWP was not entered into the multivariate analysis because of a strong correlation between PCWP and LVEDP ($\rho=0.87$).

lation between the mitral peak gradient and systolic PAP ($r=0.70$) and concluded that functional MS after RMA was strongly associated with postoperative elevated PAP and reduced exercise capacity. We found a weak but significant correlation between the mean mitral gradient and systolic PAP, which may support their speculation. However, it remains unknown whether the mitral gradient is the sole factor that affects postoperative elevated PAP.

There have been few hemodynamic studies on possible functional MS after RMA. Our hemodynamic results provide additional information about the gradients across the mitral valve and possible factors relating to postoperative PH. The present study also found a small but significant transmitral pressure gradient, calculated as the pressure difference between mean PCWP and LVEDP, which ranged from 1 to 7 mm Hg. The actual value may be slightly smaller than predicted by this pressure difference.[17] Nevertheless, about 10% of our patients (6 of 58) had a pressure gradient ≥5 mm Hg, suggesting the presence of hemodynamically substantial MS. Interestingly, in the present study, we found a strong correlation between the catheter-determined pressure gradient calculated from the mean PCWP and LVEDP, and the Doppler-derived mean gradient. This close correlation allowed us to predict the actual transmitral mean gradient, based on the pressure difference at end-diastole and to analyze relevant factors related to postoperative PH.

Hemodynamic Determinants of Postoperative PAP

Our multivariate analysis using hemodynamic variables showed that the most important determinant of systolic PAP was LVEDP, followed by PVR, and then cardiac index, whereas the contribution of the transmitral pressure gradient was the lowest of the parameters investigated. These findings suggest that the main mechanism of postoperative PH may be high LVEDP, probably due to LV systolic and diastolic dysfunction, whereas another may be pulmonary vascular disease secondary to a preoperative pulmonary hypertensive state. The contribution of a transmitral pressure gradient created by the use of an undersized ring to postoperative PH seemed relatively small in our patients.

Table 6. Preoperative Parameters Associating With Adverse Cardiac Events

	Univariate		Multivariate	
Variables	*P* Value	Hazard Ratio (95% CI)	*P* Value	Hazard Ratio (95% CI)
Clinical variables (n=108)				
Age, y	NS			
Ischemic etiology	NS			
Female	NS			
Duration of heart failure, mo	<0.001	1.01 (1.01–1.02)		
Hypertension	NS			
Diabetes	0.09	1.8 (0.9–3.6)		
Hyperlipidemia	NS			
Chronic renal failure	NS			
Peripheral vascular disease	NS			
Cerebral vascular accident	NS			
Atrial fibrillation	NS			
History of ventricular arrhythmia	0.03	2.3 (1.1–4.9)	0.04	2.1 (1.0–4.6)
Chronic obstructive pulmonary disease	NS			
Previous cardiac surgery	NS			
Preop echocardiographic parameters (n=108)				
LV end-diastolic dimension, mm	NS			
LV end-diastolic dimension >65 mm	NS			
LV end-systolic dimension, mm	0.02	1.05 (1.01–1.08)		
LV end-systolic dimension >50 mm	NS			
LV ejection fraction, %	0.006	0.94 (0.90–0.98)		
LV ejection fraction <25%	0.03	2.2 (1.1–4.3)		
Left atrial dimension, mm	NS			
RV end-diastolic dimension, mm	NS			
Systolic PAP, mm Hg*	0.04	1.02 (1.00–1.05)		
Systolic PAP >60 mm Hg	<0.001	4.6 (2.3–9.1)	<0.001	4.5 (2.2–8.9)
Preop volume and function parameters (n=97)				
LV end-diastolic volume index, mL/m^2	NS			
LV end-diastolic volume index >120 mL/m^2	NS			
LV end-systolic volume index, mL/m^2	NS			
LV end-systolic volume index >90 mL/m^2	NS			
LV ejection fraction, %	NS			
LV ejection fraction <25%	NS			
Preop hemodynamic parameters (n=75)				
LV systolic pressure, mm Hg	NS			
LVEDP, mm Hg	NS			
PCWP, mm Hg	NS			
Systolic PAP, mm Hg	NS			
Mean PAP, mm Hg	NS			
Cardiac index, $L/min/m^2$	0.07	0.6 (0.3–1.1)		
PVR, $dyne \cdot s \cdot cm^{-5}$	0.002	1.008 (1.00–1.01)		
PVR index, $dyne \cdot s \cdot cm^{-5} \cdot m^2$	0.004	1.004 (1.001–1.007)		
SVR, $dyne \cdot s \cdot cm^{-5}$	0.08	1.001 (1.000–1.002)		
SVR index, $dyne \cdot s \cdot cm^{-5} \cdot m^2$	NS			

CI indicates confidence interval; LV, left ventricular; RV, right ventricular; PAP, pulmonary artery pressure; EDP, end-diastolic pressure; PCWP, pulmonary capillary wedge pressure; PVR, pulmonary vascular resistance; SVR, systemic vascular resistance; and NS, not significant ($P>0.05$).

*Systolic PAP (continuous variable) was not entered into the multivariate analysis.

Table 7. Postoperative Parameters Associating With Adverse Cardiac Events

	Univariate		Multivariate	
Variables	*P* Value	Hazard Ratio (95% CI)	*P* Value	Hazard Ratio (95% CI)
Postop echocardiographic parameters (n=108)				
LV end-diastolic dimension, mm	0.03	1.04 (1.00–1.08)		
LV end-systolic dimension, mm	0.005	1.05 (1.01–1.08)		
LV ejection fraction, %	0.001	0.94 (0.91–0.98)		
Left atrial dimension, mm	NS			
RV end-diastolic dimension, mm	NS			
Systolic PAP, mm Hg*	<0.001	1.1 (1.04–1.13)		
Systolic PAP >40 mm Hg	<0.001	5.2 (2.6–10)	<0.001	4.6 (2.3–9.3)
Mitral valve EOA, cm^2	NS			
Indexed EOA, cm^2/m^2	NS			
Indexed EOA ≤1.2 cm^2/m^2	0.09	0.53 (0.26–1.09)		
Pressure half-time, ms	0.07	1.02 (0.99–1.04)		
Mitral mean gradient, mm Hg	0.03	1.36 (1.04–1.78)		
Mitral mean gradient ≥5 mm Hg	NS			
Residual mitral regurgitation†	NS			
Residual tricuspid regurgitation†	0.004	3.55 (1.5–8.4)	0.04	2.5 (1.0–6.1)
Surgical data (n=108)				
Ring size	NS			
Concomitant coronary artery bypass grafting	0.02	0.4 (0.2–0.8)		
Concomitant tricuspid annuloplasty	NS			
Concomitant maze procedure	NS			

CI indicates confidence interval; LV indicates left ventricular; RV, right ventricular; PAP, pulmonary artery pressure; EOA, effective orifice area; and NS, not significant ($P>0.05$).

*Systolic PAP was not entered into the multivariate analysis.

†Greater than or equal to mild grade.

Impact of the RMA Procedure on Hemodynamic and Clinical Results

The present patients with a 24-mm ring had a smaller mitral valve area and slightly greater transmitral mean gradient in echocardiographic findings, as well as a greater valve gradient in the hemodynamic evaluation, compared with those with a 26-mm ring. Despite these differences in mitral valve performance, there were no differences between the 2 groups in regard to postoperative LV volume and systolic function, PAPs, or the other measured hemodynamic parameters. Thus, in our patients, who had a lower BSA compared with those in previous studies, the use of a small prosthetic ring (24-mm Physio ring) did not appear to have a negative influence on the postoperative hemodynamic state over the short term.

Given that the normal mitral valve area is 4.0 to 5.0 cm^2, the 24- and 26-mm rings have obviously smaller orifice areas and are at least mildly obstructive to the antegrade mitral flow. The severity of this PPM can be categorized as mild, moderate, or severe according to the "in vivo" EOA indexed for the patient's BSA, as in previous studies.[7,8] Several studies have demonstrated that after mitral valve replacement, moderate PPM (indexed EOA ≤1.2 cm^2/m^2) is not uncommon, and that it has negative impacts on postoperative residual PH and late mortality and morbidity.[7,8,18] Other authors have suggested that moderate PPM in these patients is of less importance.[19,20]

In contrast, the prevalence and prognostic impact of PPM after RMA has not been well established. Our data showed that, following RMA, a considerable proportion (>20%) of patients had PPM, defined as an indexed EOA ≤1.2 cm^2/m^2. This mismatch occurred in 27% of the patients with a 24-mm ring and 12% with a 26-mm ring, which was not statistically different. Given that the pressure half-time method may overestimate the actual valve orifice area by about 10%, our in vivo EOA values suggest that the size 24- and 26-mm prosthetic rings may be too small, respectively, for patients with a BSA >1.75 to 1.80 m^2 or >1.90 to 2.00 m^2. However, it remains unclear whether such a mismatch after RMA has a negative impact on patient's prognosis.

In the present study, preoperative and postoperative residual PH, due to LV dysfunction and secondary pulmonary vascular disease, was more strongly associated with adverse cardiac events after RMA than was the severity of functional MS or the level of PPM. A Doppler-derived mean gradient of ≥5 mm Hg or an indexed EOA of ≤1.2 cm^2/m^2 did not predict adverse cardiac events during our short-term follow-up. We speculate that our identification of a negative prognostic role (a higher risk of adverse cardiac events) of this iatrogenic MS would have been masked in our analysis by the more important risk factors.

Study Limitations

The main limitation of this study is its retrospective design, as hemodynamic data could not be obtained from all of the patients, which may have resulted in a bias and restrict the statistical power of the findings. Also, in fully describing these data we have performed a large number of statistical tests, inflating the probability of making one or more type I errors across all the analyses presented. Therefore, our results should be interpreted cautiously until verified in an independent, prospective study. Furthermore, simultaneous LA and LV pressure tracings were not available, and therefore the actual mean transmitral pressure gradients and mitral valve EOA could not be determined using the Gorlin formula. In our echocardiographic and hemodynamic evaluations, the parameters were measured only in a resting condition; a dynamic exercise test with a bicycle ergometer, dobutamine stress test, or 6-minute walk test was not performed. However, data obtained from those stress tests would not have changed our conclusion. Finally, we only investigated patients who received a 24- or 26-mm Physio ring. Therefore, the results may not be applicable to patients who receive a different size or type of ring.

Conclusion

In the present study, the RMA procedure led to varying degrees of mitral valve obstruction in terms of higher transmitral mean pressure gradients (about 9% of patients) and a lesser EOA, as indexed for each patient's BSA (>20% of patients). This hemodynamic sequel was weakly associated with postoperative residual PH. However, postoperative elevated PAP was strongly associated with an elevated LVEDP and increased PVR. PH caused by LV dysfunction and pulmonary vascular disease was the most important predictor for outcomes in this study. The prognostic impact of iatrogenic MS after RMA would be hard to detect because of masking by more important risk factors.

Sources of Funding

This study was partially supported by research funds to promote the hospital function of Japan Labor Health and Welfare Organization.

Disclosures

None.

References

1. Bolling SF, Deeb GM, Brunsting LA, Bach DS. Early outcome of mitral valve reconstruction in patients with end-stage cardiomyopathy. *J Thorac Cardiovasc Surg*. 1995;109:676–683.
2. Bolling SF, Pagani FD, Deeb GM, Bach DS. Intermediate-term outcome of mitral reconstruction in cardiomyopathy. *J Thorac Cardiovasc Surg*. 1998;115:381–388.
3. Bax JJ, Braun J, Somer ST, Klautz R, Holman ER, Versteegh MI, Boersma E, Schalij MJ, van der Wall EE, Dion RA. Restrictive annuloplasty and coronary revascularization in ischemic mitral regurgitation results in reverse left ventricular remodeling. *Circulation*. 2004; 110(Suppl II):II-103–II-108.
4. Braun J, van de Veire NR, Klautz RJM, Versteegh MIM, Holman ER, Westenberg JJ, Boersma E, van der Wall EE, Bax JJ, Dion RA. Restrictive mitral annuloplasty cures ischemic mitral regurgitation and heart failure. *Ann Thorac Surg*. 2008;85:430–437.
5. Magne J, Sénéchal M, Mathieu P, Dumesnil JG, Dagenais F, Pibarot P. Restrictive annuloplasty for ischemic mitral regurgitation may induce functional mitral stenosis. *J Am Coll Cardiol*. 2008;51:1692–1701.
6. Dumesnil JG, Yoganathan AP. Valve prosthesis hemodynamics and the problem of high transprosthetic pressure gradients. *Eur J Cardiothorac Surg*. 1992;6(Suppl 1):S34–S37.
7. Li M, Dumesnil JG, Mathieu P, Pibarot P. Impact of valve prosthesis-patient mismatch on pulmonary arterial pressure after mitral valve replacement. *J Am Coll Cardiol*. 2005;45:1034–1040.
8. Magne J, Mathieu P, Dumesnil JG, Tanné D, Dagenais F, Doyle D, Pibarot P. Impact of prosthesis-patient mismatch on survival after mitral valve replacement. *Circulation*. 2007;115:1417–1425.
9. Kubota K, Otsuji Y, Ueno T, Koriyama C, Levine RA, Sakata R, Tei C. Functional mitral stenosis after surgical annuloplasty for ischemic mitral regurgitation: importance of subvalvular tethering in the mechanism and dynamic deterioration during exertion. *J Thorac Cardiovasc Surg*. 2010;140:617–623.
10. Williams ML, Daneshmand MA, Jollis JG, Horton JR, Shaw LK, Swaminathan M, Davis RD, Glower DD, Smith PK, Milano CA. Mitral gradients and frequency of recurrence of mitral regurgitation after ring annuloplasty for ischemic mitral regurgitation. *Ann Thorac Surg*. 2009;88:1197–1201.
11. Hatle L, Angelsen B, Tromsdal A. Noninvasive assessment of atrioventricular pressure half-time by Doppler ultrasound. *Circulation*. 1979;60: 1096–1104.
12. Pepi M, Tamborini G, Galli C, Barbier P, Doria E, Berti M, Guazzi M, Fiorentini C. A new formula for echo-Doppler estimation of right ventricular systolic pressure. *J Am Soc Echocardiogr*. 1994;7:20–26.
13. Kircher BJ, Himelman RB, Schiller NB. Noninvasive estimation of right atrial pressure from the inspiratory collapse of the inferior vena cava. *Am J Cardiol*. 1990;66:493–496.
14. De Bonis M, Lapenna E, Verzini A, La Canna G, Grimaldi A, Torracca L, Maisano F, Alfieri O. Recurrence of mitral regurgitation parallels the absence of left ventricular reverse remodeling after mitral repair in advanced dilated cardiomyopathy. *Ann Thorac Surg*. 2008;85:932–939.
15. Geidel S, Lass M, Schneider C, Groth G, Boczor S, Kuck KH, Ostermeyer J. Downsizing of the mitral valve and coronary revascularization in severe ischemic mitral regurgitation results in reverse left ventricular and left atrial remodeling. *Eur J Cardiothorac Surg*. 2005;27:1011–1016.
16. Gelsomino S, Lorusso R, Capecchi I, Rostagno C, Romagnoli S, Billè G, De Cicco G, Tetta C, Stefàno P, Gensini GF. Left ventricular reverse remodeling after undersized mitral ring annuloplasty in patients with ischemic regurgitation. *Ann Thorac Surg*. 2008;85:1319–1330.
17. Lange RA, Moore DM Jr, Cigarroa RG, Hillis LD. Use of pulmonary capillary wedge pressure to assess severity of mitral stenosis: is true left atrial pressure needed in this condition? *J Am Coll Cardiol*. 1989;13:825–831.
18. Lam BK, Chan V, Hendry P, Ruel M, Masters R, Bedard P, Goldstein B, Rubens F, Mesana T. The impact of patient-prosthesis mismatch on late outcomes after mitral valve replacement. *J Thorac Cardiovasc Surg*. 2007;133:1464–1473.
19. Jamieson WR, Ye J, Higgins J, Cheung A, Fradet GJ, Skarsgard P, Germann E, Chan F, Lichtenstein SV. Effect of prosthesis-patient mismatch on long-term survival with mitral valve replacement: assessment to 15 years. *Ann Thorac Surg*. 2010;89:51–58.
20. Totaro P, Argano V. Patient-prosthesis mismatch after mitral valve replacement: myth or reality? *J Thorac Cardiovasc Surg*. 2007;134:697–701.

Circulation
JOURNAL OF THE AMERICAN HEART ASSOCIATION

American Heart Association®
Learn and Live℠

Induced Adipocyte Cell-Sheet Ameliorates Cardiac Dysfunction in a Mouse Myocardial Infarction Model : A Novel Drug Delivery System for Heart Failure

Yukiko Imanishi, Shigeru Miyagawa, Norikazu Maeda, Satsuki Fukushima, Satoru Kitagawa-Sakakida, Takashi Daimon, Ayumu Hirata, Tatsuya Shimizu, Teruo Okano, Iichiro Shimomura and Yoshiki Sawa

Circulation 2011, 124:S10-S17
doi: 10.1161/CIRCULATIONAHA.110.009993
Circulation is published by the American Heart Association. 7272 Greenville Avenue, Dallas, TX 72514
 Print ISSN: 0009-7322. Online ISSN: 1524-4539

Induced Adipocyte Cell-Sheet Ameliorates Cardiac Dysfunction in a Mouse Myocardial Infarction Model

A Novel Drug Delivery System for Heart Failure

Yukiko Imanishi, PhD; Shigeru Miyagawa, MD, PhD; Norikazu Maeda, MD, PhD; Satsuki Fukushima, MD, PhD; Satoru Kitagawa-Sakakida, MD, PhD; Takashi Daimon, PhD; Ayumu Hirata, MD, PhD; Tatsuya Shimizu, MD, PhD; Teruo Okano, PhD; Iichiro Shimomura, MD, PhD; Yoshiki Sawa, MD, PhD

Background—A drug delivery system that constitutively and effectively retains cardioprotective reagents in the targeted myocardium has long been sought to treat acute myocardial infarction. We hypothesized that a scaffold-free induced adipocyte cell-sheet (iACS), transplanted on the surface of the heart, might intramyocardially secrete multiple cardioprotective factors including adiponectin (APN), consequently attenuating functional deterioration after acute myocardial infarction.

Methods and Results—Induced ACS were generated from adipose tissue–derived cells of wild-type (WT) mice (C57BL/6J), which secreted abundant APN, hepatocyte growth factor, and vascular endothelial growth factor in vitro. Transplanted iACS secreted APN into the myocardium of APN-knockout (KO) mice at 4 weeks. APN was also detected in the plasma of iACS-transplanted APN-KO mice at 3 months (245±113 pg/mL). After left anterior descending artery ligation, iACS, generated from either WT (n=40) or APN-KO (n=40) mice, were grafted onto the surface of the anterior left ventricular wall of WT mice, or only left anterior descending artery ligation was performed (n=43). Two days later, inflammation and infarct size were significantly diminished only in the WT-iACS treated mice. One month later, cardiomyocyte diameter and percent fibrosis were smaller, whereas ejection fraction and survival were greater in the WT-iACS treated mice compared with the KO-iACS–treated or nontreated mice.

Conclusions—Cardioprotective factors including APN, hepatocyte growth factor, and vascular endothelial growth factor were secreted from iACS. Transplantation of iACS onto the acute myocardial infarction heart attenuated infarct size, inflammation, and left ventricular remodeling, mediated by intramyocardially secreted APN in a constitutive manner. This method might be a novel drug delivery system to treat heart disease. **(*Circulation*. 2011;124[suppl 1]:S10–S17.)**

Key Words: acute myocardial infarction ■ adiponectin ■ cell therapy ■ drug delivery system ■ tissue engineering

Despite recent progress in medical and surgical treatments for heart failure, acute myocardial infarction (AMI) and the subsequent deterioration of cardiac performance is still a major cause of death, worldwide. An array of cardioprotective reagents have been identified to be effective in ameliorating AMI by administrating into the infarcted myocardium in experimental models.[1] However, these reagents have failed to show consistent therapeutic efficacy in several clinical trials, probably due to poor retention or rapid inactivation of reagents in the injured myocardial tissues.[1] Therefore, a drug delivery system (DDS) that retains cardioprotective reagents in the targeted myocardial area has long been sought.

Intramyocardially transplanted autologous stem cells secrete various cardioprotective cytokines and growth factors, enhance angiogenesis, reduce fibrosis, attenuate apoptosis, and suppress myocyte hypertrophy, consequently ameliorating AMI in a paracrine manner.[2,3] However, cell transplantation for AMI has shown only modest therapeutic efficacy in large-scale clinical studies. It appears to result from insufficient paracrine effects whose magnitude and figure are largely affected by the cell delivery method or transplanted cell source.[4] To enhance the survival and functions of the transplanted cells, we developed a cell-sheet–based delivery method in which isolated cells, cultivated in vitro as a sheet without a scaffold, are simply placed on the surface of the myocardium. This treatment enhances the paracrine effects, resulting in better therapeutic efficacy.[5,6]

Adipocytes differentiated from adipose tissue–derived stromal-vascular fraction (SVF) cells are a promising cell

From the Department of Cardiovascular Surgery (Y.I., S.M., S.F., S.K.-S., Y.S.) and the Department of Metabolic Medicine (N.M., A.H., I.S.), Graduate School of Medicine, Osaka University, Suita, Osaka, Japan; the Division of Biostatistics (T.D.), Department of Mathematics, Hyogo College of Medicine, Nishinomiya, Hyogo, Japan; and the Institute of Advanced Biomedical Engineering and Science (T.S., T.O.), Tokyo Women's Medical University, Shinjuku-ku, Tokyo, Japan.

Presented at the 2010 American Heart Association meeting in Chicago, IL, November 12–16, 2010.

The online-only Data Supplement is available at http://circ.ahajournals.org/lookup/suppl/doi:10.1161/CIRCULATIONAHA.110.009993/-/DC1.

Correspondence to Yoshiki Sawa, 2-2 Yamada-oka, Suita City, Osaka 565-0871, Japan. E-mail sawa@surg1.med.osaka-u.ac.jp

Circulation **is available at http://circ.ahajournals.org** **DOI: 10.1161/CIRCULATIONAHA.110.009993**

source for treating AMI because as they secrete hepatocyte growth factor (HGF), vascular endothelial growth factor (VEGF), and, importantly, adiponectin (APN).[7,8] APN is a circulating secretory protein that has multiple cardioprotective effects, including the attenuation of inflammation, fibrosis, and myocyte hypertrophy.[8,9] However, the clinical use of APN for treating AMI has been hampered by the lack of effective systems for delivering APN to the heart. We hypothesized that using cell-sheet technology to deliver adipocytes that secrete multiple cardioprotective factors, including APN, might attenuate the functional deterioration after AMI.

Methods

Animal care complied with the "Guide for the Care and Use of Laboratory Animals" (NIH publication No. 85 to 23, revised 1996). Experimental protocols were approved by the Ethics Review Committee for Animal Experimentation of Osaka University Graduate School of Medicine.

Generation and Assessment of Adipocyte Cell-Sheet

The SVF cells of adipose tissue were isolated from wild-type (WT; male C57BL/6J) or APN-knockout (KO) mice,[10] as described previously.[11] The isolated SVF cells were cultured until they become confluent on Upcell dishes (CellSeed Inc, Tokyo, Japan). Differentiation into adipocytes was induced by insulin, dexamethasone, isobutylmethylxanthine, and pioglitazone (Sigma-Aldrich, MO). Incubation at 20°C induced the cells to detach from the culture dishes, yielding a scaffold-free cell-sheet, which we call an "induced adipocyte cell-sheet" (iACS). The secretion of HGF, VEGF, leptin, interleukin (IL)-6, tumor necrosis factor (TNF)-α, and IL-10 into the culture supernatant was assessed by ELISA. Before transplantation, WT mouse–derived iACS (WT-iACS) and APN-KO mouse–derived iACS (KO-iACS) were labeled with the use of a PKH26 kit (Sigma-Aldrich).

Generation of AMI Model and Cell-Sheet Transplantation

An AMI model was generated by permanent ligation of the left anterior descending artery (LAD) in male C57BL/6J mice, 10 to 15 weeks old.[12] The mice were anesthetized by isoflurane inhalation (Mylan Inc). Five minutes after the LAD ligation, WT-iACS (W group, n=40) or KO-iACS (K group, n=40) was grafted onto the surface of the anterior left ventricular (LV) wall, or a sham operation was performed (C group, n=43). The mice were euthanized at 2 and 28 days after LAD ligation and cell-sheet transplantation.

Assessment of Cardiac Function and Survival

Cardiac function was assessed with the use of an echocardiography system equipped with a 12-MHz transducer (GE Healthcare) at 4 weeks. The LV dimensions were measured, and LV ejection fraction was calculated as $(LVDd^3-LVDs^3)/LVDd^3\times100$, where LVDd and LVDs are the LV end-diastolic and end-systolic dimensions, respectively.[12] The mice were housed in a temperature-controlled incubator for 50 days after treatment to determine their survival.

Histological Analysis

Freshly excised hearts were stained with 1% 2,3,5-triphenyltetrazolium chloride (TTC; Sigma-Aldrich). The red-stained infarct area was quantified by computerized planimetry, using MetaMorph Software (Molecular Devices). Frozen sections (8 μm) of hearts and cell-sheets were stained with antibodies against APN (Otsuka Pharmaceutical, Tokushima, Japan) or CD11b (Abcam, Cambridge, UK). The secondary antibody was Alexa 488 goat anti-rabbit (Life Technologies). Counterstaining was performed with 6-diamidino-2-phenylindole (Life Technologies). To analyze the myocardial collagen accumulation, heart sections were stained with Masson trichrome. The collagen volume fraction was calculated in the peri-infarct area. To assess cardiomyocyte diameter, heart sections were stained with periodic acid-Schiff. MetaMorph Software was used for the quantitative morphometric analysis.

Cytokine Antibody Array

Proteins were isolated from whole-heart samples and analyzed using a Milliplex Mouse Cytokine/Chemokine Panel Premixed 32Plex, according to the manufacturer's instructions (Millipore).

Quantitative Real-Time PCR

Total RNA was isolated from the peri-infarct area by use of the RNeasy Mini Kit and reverse-transcribed, using Omniscript Reverse transcriptase (Qiagen, Hilden, Germany). Quantitative PCR was performed with the PCR System (Life Technologies). The expression of each mRNA was normalized to that of glyceraldehyde-3-phosphate dehydrogenase.

Statistical Analysis

Data are expressed as the mean±SEM. The data distributions were checked for normality with the Shapiro-Wilk test and for equality of variances with the Bartlett test. Comparisons between 2 groups were made using the unpaired t test or the Wilcoxon-Mann-Whitney U test, as appropriate. For comparisons among 3 groups, we used 1-way ANOVA, followed by Fisher protected least-significance difference test or the Kruskal-Wallis test, followed by the post hoc pairwise Wilcoxon-Mann-Whitney U test, as appropriate. The survival curves were prepared by using the Kaplan-Meier method and were compared using the overall log-rank test, followed by the post hoc pairwise log-rank test. The multiplicity in pairwise comparisons was corrected by the Benjamin-Hochberg procedure. All probability values are 2-sided, and values of $P<0.05$ were considered to indicate statistical significance. Statistical analysis was performed with the StatView 5.0 Program (Abacus Concepts, Berkeley, CA) and the R program.[13]

An expanded Methods section can be found in the online-only Data Supplement.

Results

Characterization of the Adipocyte Cell-Sheets

Most SVF cells differentiated into mature adipocytes bearing oil droplets by 7 days after differentiation induction. Induced ACS or undifferentiated SVF cell-sheets were then generated by lowering the temperature (Figure 1A). Each iACS was approximately 7 mm in diameter (Figure 1B) and 100 μm thick (Figure 1C). WT-iACS expressed abundant APN in the cytoplasm and extracellular matrix around the oil-droplet–rich adipocytes, as assessed by immunohistochemistry (Figure 1D) and ELISA (Figure 1E). In contrast, neither the SVF cell-sheets of either origin nor the KO-iACS expressed APN (Figure 1D and 1E). The ELISA showed abundant HGF expression in WT-iACS and KO-iACS, which was down-regulated compared with the WT SVF cells (Figure 1F). The secretion of VEGF and leptin was remarkably enhanced by the SVF cell differentiation into adipocytes. IL-6 and IL-10 were secreted by the WT-iACS and WT-SVF cells at similar levels, which were lower than the levels secreted by KO-iACS. The secretion of TNF-α was not evident in any group because the cell-free culture medium also contained 2.29 pg/mL TNF-α.

Transplanted Induced ACS Supplied APN to the Myocardium

WT-iACS were transplanted onto the heart of intact APN-KO mice to evaluate behavior of the WT-iACS, including APN

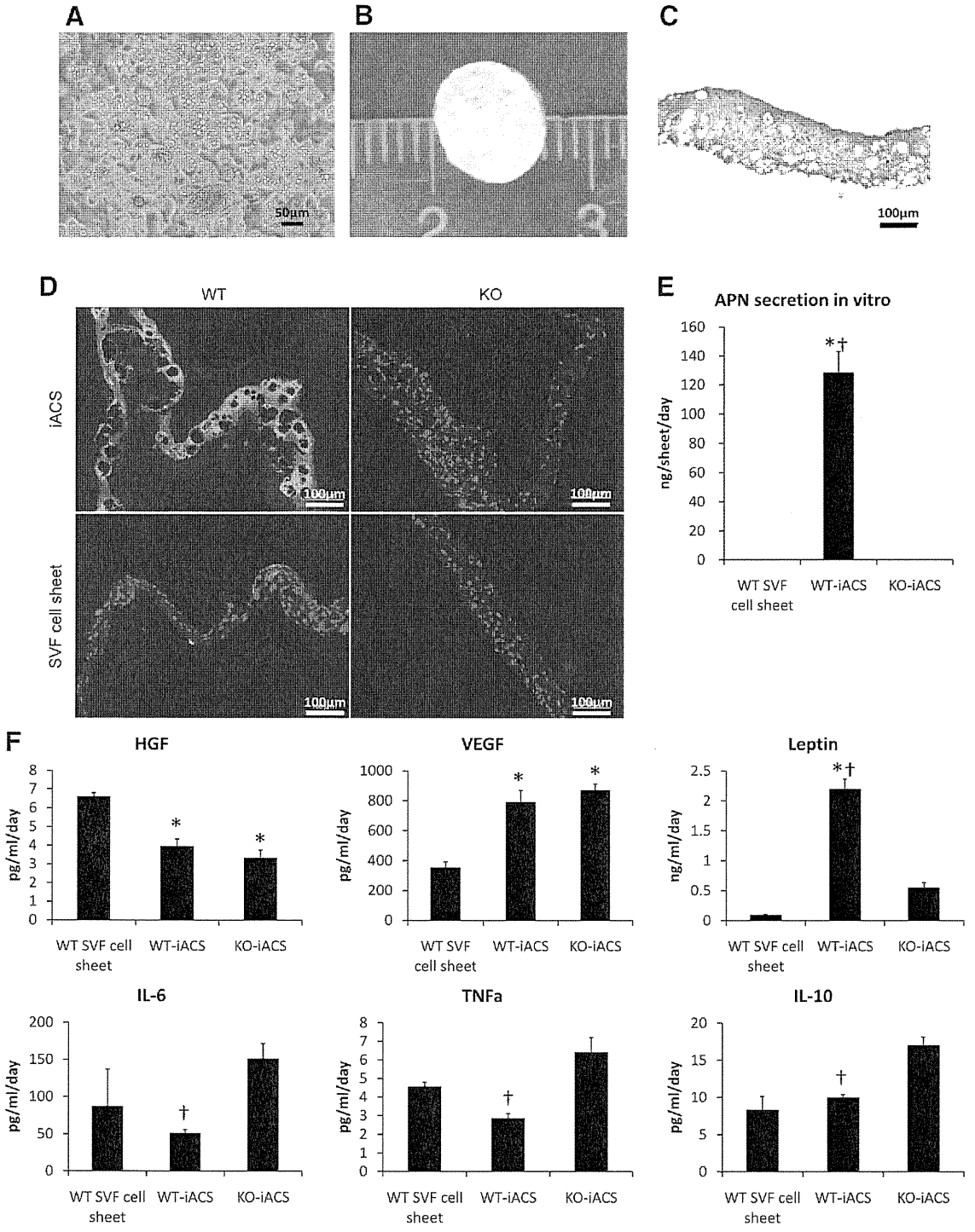

Figure 1. Characterization of induced adipocyte cell-sheet (iACS) in vitro. **A**, Histological analysis showing mature adipocytes with oil droplets in the cytosol. **B**, Induced ACS detached from the temperature-responsive culture dish. **C**, Cross-sectional view of hematoxylin and eosin–stained iACS. **D**, Representative pictures of adiponectin (APN)-stained cell-sheets. Wild-type (WT)-iACS showed strong labeling for APN. The WT stromal-vascular fraction (SVF) cell-sheet, knockout (KO)-iACS, and KO SVF cell-sheet were negative for APN. Green indicates APN; blue, nuclei. **E**, APN secretion into the WT-iACS culture supernatant determined by ELISA (WT SVF cell sheet, n=2; WT-iACS, n=5; KO-iACS, n=8; $P<0.05$, Kruskal-Wallis test). *$P<0.05$ versus WT SVF cell-sheet, †$P<0.05$ versus KO-iACS, post hoc Wilcoxon-Mann-Whitney *U* test. **F**, Hepatocyte growth factor (HGF), vascular endothelial growth factor (VEGF), leptin, interleukin (IL)-6, IL-10, and tumor necrosis factor (TNF)-α secretion into the culture supernatant, measured by ELISA. WT-iACS secreted HGF, VEGF, leptin, IL-6, and IL-10 but not TNF-α (WT SVF cell sheet, n=2; WT-iACS, n=8 to 12; KO-iACS, n=6 to 9). HGF, VEGF, and leptin ($P<0.05$, ANOVA); *$P<0.05$ versus WT SVF cell-sheet, †$P<0.05$ versus KO-iACS, post hoc Fisher protected least-significance difference test. TNF-α, IL-6, and IL-10 ($P<0.05$, Kruskal-Wallis test); *$P<0.05$ versus WT SVF cell-sheet, †$P<0.05$ versus KO-iACS, post hoc Wilcoxon-Mann-Whitney *U* test.

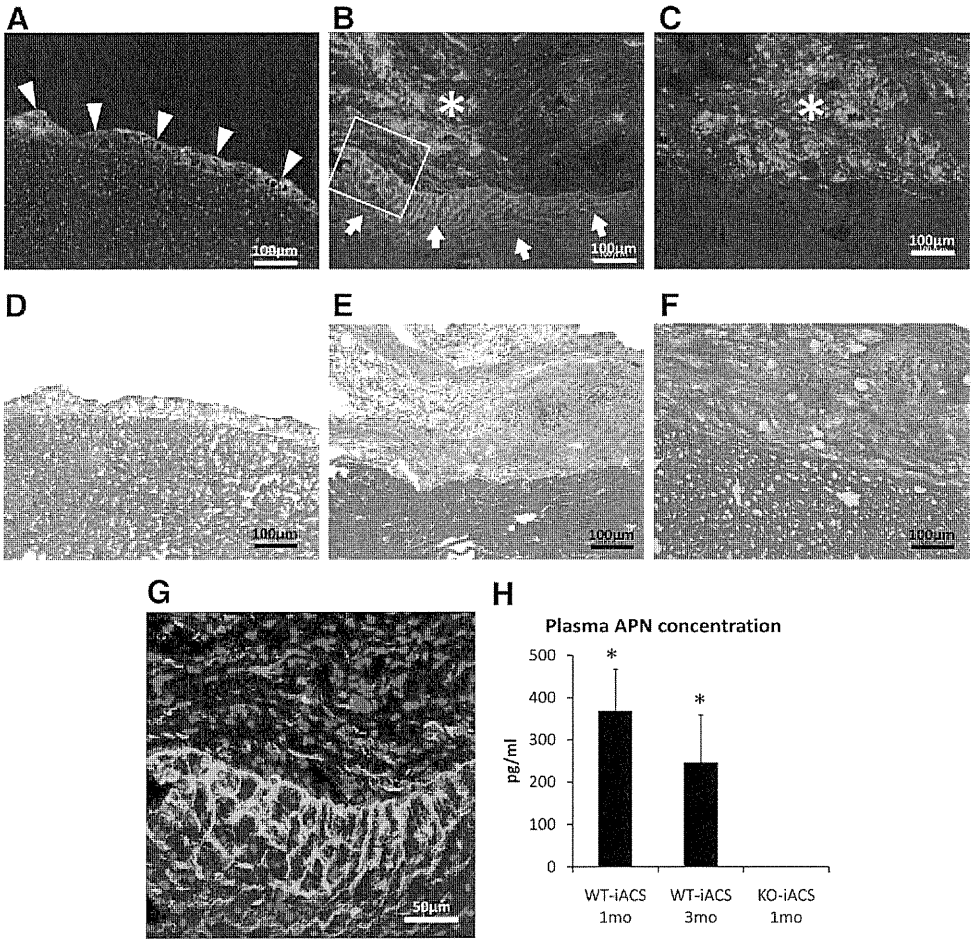

Figure 2. Local and systemic delivery of induced adipocyte cell-sheet (iACS)-derived adiponectin (APN) in vivo. **A**, Immediately after wild-type (WT)-iACS implantation onto the knockout (KO) mouse heart, iACS-expressed APN was detected on the epicardium. Arrowheads show the implanted WT-iACS. Green indicates APN; blue, nuclei. **B**, WT-iACS stained with red fluorescent dye were implanted onto KO myocardium. Twenty-eight days after transplantation, APN was detected both in the surviving WT-iACS and the extracellular matrix (ECM) of the KO mouse myocardium at the implanted site. Asterisk indicates the implanted WT-iACS. Arrows show iACS-derived APN in the host myocardium. **C**, KO-iACS stained with red fluorescent dye and implanted onto KO myocardium. Twenty-eight days after transplantation, the implanted KO-iACS survived, but no APN was detected in the KO-iACS or the ECM. Asterisk indicates the implanted KO-iACS. Green indicates APN; red, KO-iACS; and blue, nuclei. **D** through **F**, Hematoxylin and eosin staining of a serial section from the sample in **A**, **B**, and **C**, respectively. **G**, High-magnification image of the square in **B** and **H**. Plasma APN concentration of WT-iACS (WT) or KO-iACS (KO) recipient APN-KO mice. APN was detected in the WT group plasma 1 (n=4) and 3 months (n=3) after transplantation but not in the KO group plasma (n=4, $P<0.05$, Kruskal-Wallis test). *$P<0.05$ versus KO 1 month, post hoc Wilcoxon-Mann-Whitney *U* test.

production. Immediately after transplantation, the WT-iACS expressed APN epicardially at the anterior LV wall, but it was not expressed intramyocardially (Figure 2A). Four weeks after transplantation, the WT-iACS had survived, was approximately 600 μm thick, and contained adipocytes and connective tissue. At this time, the WT-iACS was tightly integrated with the epicardium, but no invasion of transplanted cells into the recipient myocardium was observed (Figure 2B and 2E). APN was expressed in the cytoplasm of scattered surviving WT-iACS cells and in the myocardium close to the WT-iACS (Figure 2B and 2G). In contrast, although the KO-iACS transplanted into KO mice survived (Figure 2C and 2F), they did not express or secrete APN (Figure 2C). When WT-iACS was transplanted into KO mice, APN was detected in the plasma 1 and 3 months later, but it was not detected in the plasma of KO mice with the KO-iACS implant (Figure 2H).

Induced ACS Implantation Reduced Inflammatory Responses and Infarct Area 2 Days After MI

The anti-inflammatory effects of WT-iACS were evaluated by cytokine antibody array analysis of whole-heart lysates from the AMI mice that were treated with WT-iACS (W), KO-iACS (K), or no iACS (C) groups at 2 days after implantation (Table). A significantly lower level of the inflammatory factor granulocyte macrophage colony-stimulating factor (GM-CSF) was observed in the W group compared with the others, and the levels of other inflammatory cytokines, keratinocyte chemoattractant, IL-6, granulocyte (G)-CSF, and monocyte chemotactic protein-1 (MCP-1) showed a trend toward downregulation in the W group. Quantitative RT-PCR showed that the TNFα mRNA levels were lower in the peri-infarct area of the W group than in that of the K and C groups, which reached statistical significance in the W group (Figure 3A). Furthermore, immunohistochem-

Table. Cytokine Antibody Array

	W Group (n=4)	K Group (n=5)	C Group (n=6)
Granulocyte macrophage colony-stimulating factor, pg	0.0±0*†	21.8±1.3	18.5±6.7
Keratinocyte chemoattractant, pg	292.7±42.7	539.9±56.4	629.9±113.1
Interleukin-6, pg	175.3±16.0	295.3±44.0	281.4±51.5
Granulocyte-colony stimulating factor, pg	37.6±5.7	94.6±35.0	52.8±9.5
Monocyte chemotactic protein-1, pg	316.4±51.9	467.6±50.4	388.7±87.1

$P<0.05$, Kruskal-Wallis test.
*$P<0.05$ versus C group.
†$P<0.05$ versus K group, post hoc Wilcoxon-Mann-Whitney U test.

istry for CD11b showed significantly fewer infiltrated macrophages in the peri-infarct area of the W and K groups than in that of the C group (Figure 3B). Finally, a semiquantitative assessment by TTC staining showed that the infarct area was significantly smaller in the W group than in the K and C groups (Figure 4).

Induced ACS Transplantation Suppressed LV Remodeling Development at 4 Weeks After MI

Four weeks after LAD ligation, the C group showed a typical MI with a large anterior LV scar, dilatation of the LV cavity, and cardiomyocyte hypertrophy. By comparison, the LV of the W group was less dilated, and the anterior wall was thicker (Figure 5A). The diameter of the cardiomyocytes was significantly smaller in the W group (Figure 5B and 5C), and there was less collagen accumulation (Figure 5D and 5E). There was no difference in capillary density among the groups (online-only Data Supplement Figure 1).

Therapeutic Effects of Induced ACS Transplantation on Cardiac Performance and Survival at 4 Weeks After MI

Cardiac performance was evaluated by 2D echocardiography 4 weeks after implantation. Both the diastolic and systolic LV dimensions were smaller in the W group than the others, but the difference was not significant. In contrast, LV ejection fraction was significantly greater in the W group than the K and C groups (Figure 6A). In addition, in a WT-iACS–transplanted rat model of acute MI, invasive hemodynamic analysis showed higher end-systolic pulmonary vascular resistance and dP/dtmax and lower dP/dtmin, compared with sham transplantation (online-only Data Supplement Figure 2). Mortality was substantial until 14 days after LAD ligation in the K and C groups. In contrast, in the W group, there was little mortality 5 days after MI and thus a significant difference in survival (Figure 6B).

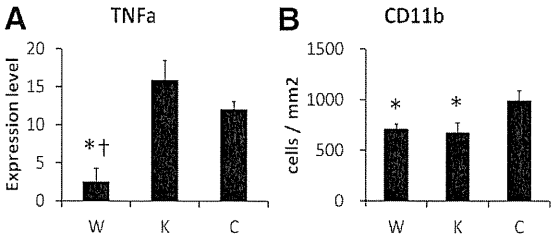

Figure 3. Induced adipocyte cell-sheet (iACS) effects on inflammatory responses after myocardial infarction at the implant/myocardium border zone 2 days after implantation. **A**, Quantitative RT-PCR results for the tumor necrosis factor (TNF)-α transcript. TNF-α transcription was significantly lower in the W group (n=4) than in the K (n=4) and C groups (n=6, $P<0.05$, Kruskal-Wallis test) *$P<0.05$ versus C group, †$P<0.05$ versus K group, post hoc Wilcoxon-Mann-Whitney U test. **B**, Quantification of CD11b-positive cells. The number of CD11b-positive cells was significantly lower in the W (n=4) and K (n=4) groups than in the C group (n=6, $P<0.05$, ANOVA). *$P<0.05$ versus C group, Fisher protected least-significance difference test.

Discussion

We developed an adipocyte cell-sheet–based DDS for the heart. These sheets, which are generated from adipose tissue–derived SVF cells induced to differentiate in culture, secreted multiple cardioprotective factors in vitro, including APN, HGF, and VEGF. Although adipose tissue–derived SVF cells had no ability to secrete APN, after the differentiation to adipocytes, the cells started to secrete APN in addition to HGF and VEGF. APN was secreted from the iACS into the myocardium and blood for at least 3 months, probably along with HGF, VEGF, leptin, and IL-10. In a mouse model of AMI, WT-iACS significantly decreased inflammation and myocardial infarct size at the acute stage. Furthermore, myocardial fibrosis and cardiomyocyte hypertrophy were significantly attenuated at the late stage, which led to improved cardiac performance and a better post-MI survival rate. Importantly, the transplantation of KO-iACS onto infarcted hearts resulted in only modest therapeutic benefits, indicating that APN plays a pivotal role in attenuating the AMI in this experimental model.

There have been many experimental and clinical studies in which the administration of exogenous proteins, including APN, induced angiogenesis, reversed remodeling, and improved cardiac function.[1,14] The issues in this method may be that naked protein is delivered to the heart and is often poorly retained or quickly inactivated and therefore lacks long-term efficacy.[15] MI is a progressive disease, characterized by massive ischemic necrosis of the myocardial tissue and subsequent inflammation. This leads to cardiac remodeling that exacerbates the oxygen shortage in the surviving cardiac tissue. These pathological and functional deteriorations eventually cause end-stage heart failure. A constitutive and balanced supply of cardioprotective reagents, rather than the 1-time administration of a single reagent, should inhibit this vicious circle. The direct injection of plasmid vectors encoding targeted reagents and the transplantation of genetically modified cells can provide a controlled and stable supply of reagents over the long term; however, their clinical use is limited because the safety of the viral systems used as vectors for the plasmids and of modifying cells for transplant is still a concern.[16] Encapsulation as the DDS for biomaterials is another attractive approach; however, difficulty in controlling the rate of reagent release, such as the occurrence of an initial burst release, limits its therapeutic efficacy.[17,18] In addition, biodegradable polymers that carry reagents may induce the deposition of extracellular matrix and myocardial inflamma-

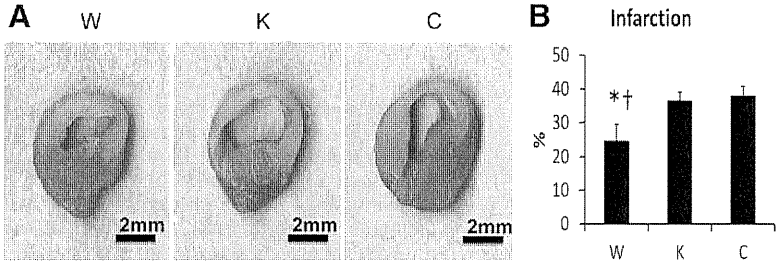

Figure 4. Infarct area of induced adipocyte cell-sheet (iACS)-treated heart 2 days after myocardial infarction. **A**, Representative 2,3,5-triphenyltetrazolium chloride staining images at border zone of infarct. **B**, Quantification of infarct size. The percent infarcted area was significantly lower in the W group (n=8) compared with the other groups (K, n=7; C, n=9; $P<0.05$, ANOVA). *$P<0.05$ versus C group. †$P<0.05$ versus K group, Fisher protected least-significance difference test.

tion, leading to pathological fibrotic states.[19] Our cell-sheet–based DDS constitutively and effectively delivered multiple cardioprotective factors over the long term, leading to reverse LV remodeling after MI, without gene modification or scaffold use. Thus, this strategy might be more practical and effective than other methods for delivering therapeutic proteins for treating MI in the clinical arena.

It is possible that the delivery of multiple growth factors will improve therapeutic efficacy over the delivery of a single factor. This hypothesis is supported by a study showing that the combination of HGF and VEGF leads to better engraftment and significant angiogenesis, compared with either factor alone.[20] In our study, the KO-iACS, which secreted HGF and VEGF but not APN, reduced macrophage infiltration but did not induce functional or survival benefits. These benefits were conferred by the WT-iACS, which produced APN, suggesting that APN's benefits are different from and in addition to those of known paracrine mediators, such as HGF or VEGF.

APN is a protective factor against cardiovascular diseases.[9,21] In particular, its anti-inflammatory properties may be the major reason for its beneficial effects on cardiovascular disorders, because APN-deficient mice exhibit increased TNF-α production and myocardial apoptosis in response to ischemia reperfusion.[22,23] We observed that the expression of TNF-α in the AMI heart was significantly reduced by transplanting WT-iACS but not KO-iACS, which secrete similar levels of the same cytokines, except for APN, suggesting that the direct anti-inflammatory effects of APN played a key role in the attenuated inflammation in this study. In addition, the infarct size was significantly smaller in the WT-iACS–transplanted hearts than in the KO-iACS–transplanted ones. Infarct size is determined by multiple factors, including the magnitude of ischemic stimuli, degree of

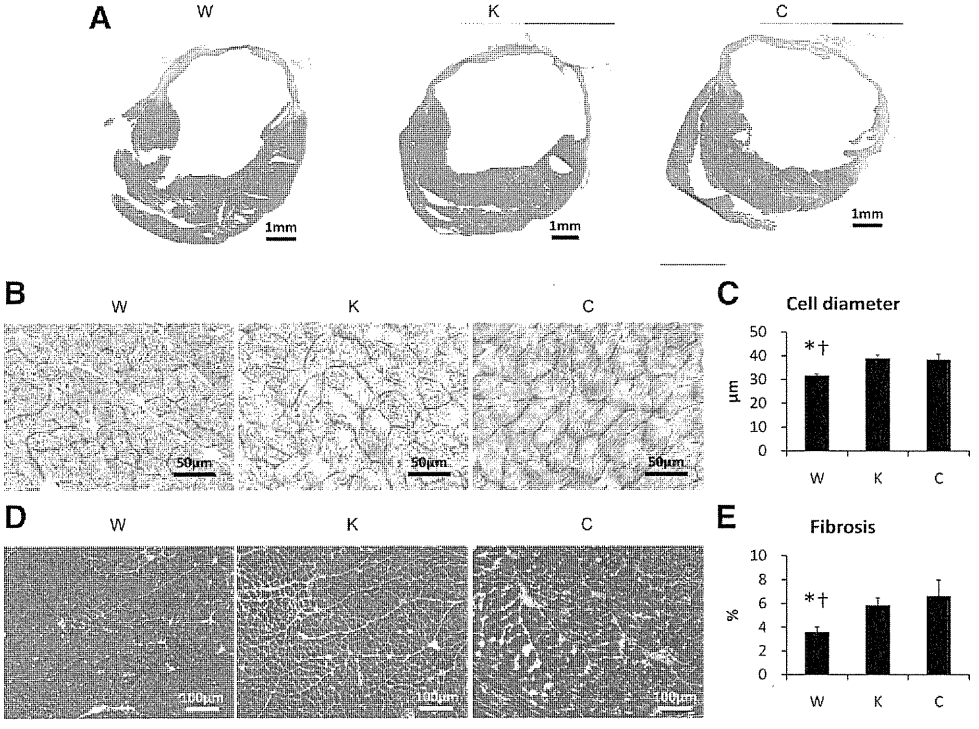

Figure 5. Effects on left ventricular remodeling by induced adipocyte cell-sheet (iACS) transplantation 4 weeks after myocardial infarction. **A**, Representative macro images from each group. **B**, Representative periodic acid-Schiff staining of tissue remote from infarct site. **C**, Quantification of cardiomyocyte diameter. Cardiomyocyte diameters in the tissue remote from the infarct site were significantly smaller in the W group (n=6) than in the other groups (K, n=8; C, n=5; $P<0.05$, ANOVA). *$P<0.05$ versus C group. †$P<0.05$ versus K group, Fisher protected least-significance difference test. **D**, Representative Masson trichrome staining images at the border area. **E**, Quantification of percent fibrosis. Fibrosis at the border area was significantly suppressed in the W group (n=6) compared with the other groups (K, n=8; C, n=5; $P<0.05$, Kruskal-Wallis test). *$P<0.05$ versus C group. †$P<0.05$ versus K group, post hoc Wilcoxon-Mann-Whitney *U* test.

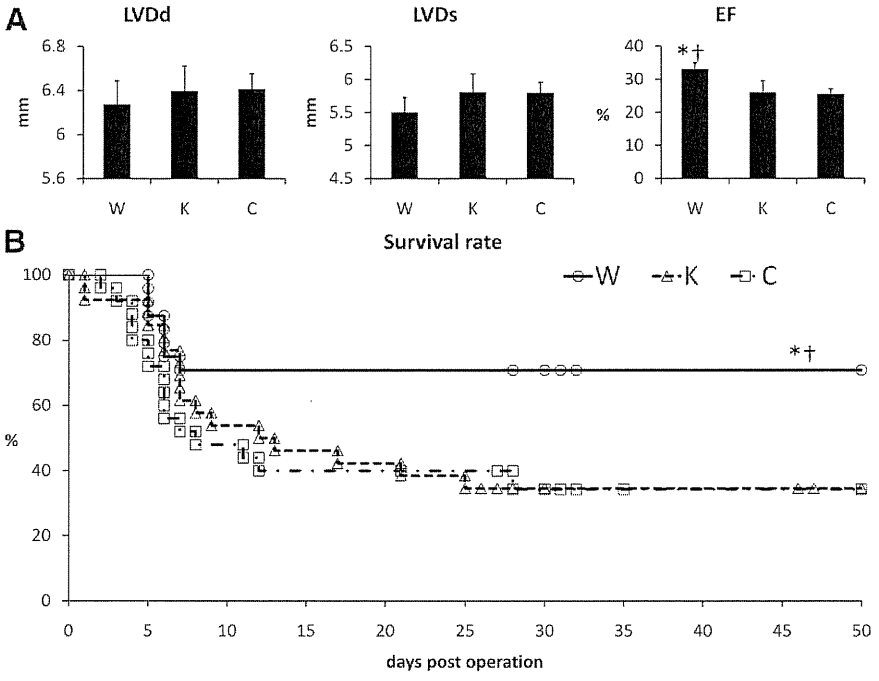

Figure 6. Wild-type induced adipocyte cell-sheet (WT-iACS) improved cardiac function and survival after myocardial infarction. **A**, Evaluation of cardiac performance 4 weeks after treatment (n=18 each). In the W group, the left ventricular end-systolic dimension was smaller and the ejection fraction significantly higher than in the other groups ($P<0.05$, Kruskal-Wallis test). *$P<0.05$ versus C group. †$P<0.05$ versus K group, post hoc Wilcoxon-Mann-Whitney U test. **B**, Survival rates after treatment. There was no significant difference between the C (n=25) and K groups (n=26). The W group (n=24) showed significantly better survival than the other groups ($P<0.05$, overall log-rank test). *$P<0.05$ versus C group, †$P<0.05$ versus K group, post hoc log-rank test.

inflammation, and amount of apoptosis. The beneficial effects of APN on inflammation after the iACS treatment may have led to the attenuated infarct size and suppressed the exacerbation of cardiac performance. In addition, APN has been shown to directly inhibit the hypertrophic response in myocytes.[24] Therefore, the combined direct and indirect actions of APN probably inhibit the development of pathological hypertrophy and preserve myocardial mass. Although we traced the iACS-derived APN by using APN-KO mice to demonstrate the APN delivery, HGF, VEGF, and other beneficial growth factors are probably also released constitutively by the iACS. Thus, iACS can provide a combined and balanced release of multiple paracrine mediators that may synergistically augment therapeutic benefits.[20,23]

On the other hand, APN is reported to have proangiogenic potential.[9] In fact, VEGF secretion from WT-iACS and KO-iACS were also greater compared with undifferentiated WT-SVF cell-sheet in this study. However, the capillary density in the treated myocardium, which was assessed by CD31 immunohistolabeling, was not higher at 28 days after WT-iACS transplantation, compared with post–KO-iACS transplantation and sham transplantation. These inconsistent findings may result from the AMI model in which neoangiogenesis substantially occurs in the treated area, not allowing dissection of the slight difference in capillary density between the experimental groups. Rather, the findings of this study suggested that anti-inflammatory effects were the major mechanism for the improvement after WT-iACS transplantation in this model. Another disease model such as dilated cardiomyopathy and old myocardial infarction may be more appropriate to evaluate angiogenic property of iACS treatment.

The treatment strategy for AMI studied here is not directly applicable to the clinical arena, because the time required to isolate, cultivate, or manipulate cells in vitro is not available for AMI, which requires immediate treatment. However, the finding that this therapy yielded marked cardioprotective effects through constitutive APN production should be beneficial for treating other types of cardiac pathologies, such as the chronic phase of MI, dilated cardiomyopathy, or myocarditis. In addition, this sophisticated cell-sheet, which elevates the systemic APN level for some time, might also be effective for treating systemic disorders such as obesity-linked cardiovascular or metabolic disorders, although this possibility will require further investigation.[9,21]

A potential limitation of this study is that the small sample sizes in our experiments limit their statistical power. Thus, the apparent absence of a statistical difference may be due to the lack of statistical power to detect small differences; therefore our negative results may have no meaning. Nevertheless, despite the small sample sizes, we at least clearly showed that APN was delivered by WT-iACS and that the therapeutic effect of WT-iACS implantation was attained through APN. Furthermore, we conducted multiple statistical tests for significance separately for each outcome in a univariate manner, although we adjusted for multiple pairwise testing between groups within each outcome. Such tests for multiple outcomes could lead to the inflation of the type I error probability in making treatment effect claims.

In the present study, we focused on the delivery of cytokines by iACS. However, we speculate that other mechanisms may also contribute to the functional recovery after iACS implantation. Tateno et al[25] clearly showed that cell transplantation induces the recipient tissue to produce angiogenic factors, including IL-1β, even though the transplanted cells do not produce sufficient levels of cytokines to promote angiogenesis directly. Similarly, iACS may stimulate recipient tissue, thus activating cells in the recipient to produce angiogenic cytokines. Further study will be required to elucidate what cross-talk occurs between the iACS and the recipient myocardium.

In summary, iACS may be a powerful DDS for cytokines, including APN, HGF, and VEGF. The implantation of iACS onto the infarcted mouse heart reduces the infarct size, inflammation, and LV remodeling. This method is probably adaptable as a novel DDS for treating heart failure.

Acknowledgments

We thank Masako Yokoyama and Yoko Motomura for excellent technical assistance.

Sources of Funding

This study was funded in part by a grant-in-aid for Scientific Research (22659251) from the Ministry of Education, Culture, Sports, Science, and Technology of Japan.

Disclosures

Dr Shimizu is a consultant for CellSeed, Inc. Dr Okano is an Advisory Board Member in CellSeed, Inc, and an inventor/developer designated on the patent for temperature-responsive culture surfaces.

References

1. Hwang H, Kloner RA. Improving regenerating potential of the heart after myocardial infarction: factor-based approach. *Life Sci.* 2010;86:461–472.
2. Vandervelde S, van Luyn MJ, Tio RA, Harmsen MC. Signaling factors in stem cell-mediated repair of infarcted myocardium. *J Mol Cell Cardiol.* 2005;39:363–376.
3. Gnecchi M, Zhang Z, Ni A, Dzau VJ. Paracrine mechanisms in adult stem cell signaling and therapy. *Circ Res.* 2008;103:1204–1219.
4. Herrmann JL, Abarbanell AM, Weil BR, Wang Y, Wang M, Tan J, Meldrum DR. Cell-based therapy for ischemic heart disease: a clinical update. *Ann Thorac Surg.* 2009;88:1714–1722.
5. Miyagawa S, Saito A, Sakaguchi T, Yoshikawa Y, Yamauchi T, Imanishi Y, Kawaguchi N, Teramoto N, Matsuura N, Iida H, Shimizu T, Okano T, Sawa Y. Impaired myocardium regeneration with skeletal cell sheets–a preclinical trial for tissue-engineered regeneration therapy. *Transplantation.* 2010;90:364–372.
6. Shimizu T, Sekine H, Yamato M, Okano T. Cell sheet-based myocardial tissue engineering: new hope for damaged heart rescue. *Curr Pharm Design.* 2009;15:2807–2814.
7. Nakagami H, Morishita R, Maeda K, Kikuchi Y, Ogihara T, Kaneda Y. Adipose tissue-derived stromal cells as a novel option for regenerative cell therapy. *J Atheroscler Thromb.* 2006;13:77–81.
8. Maeda K, Okubo K, Shimomura I, Funahashi T, Matsuzawa Y, Matsubara K. CDNA cloning and expression of a novel adipose specific collagen-like factor, apm1 (adipose most abundant gene transcript 1). *Biochem Biophys Res Commun.* 1996;221:286–289.
9. Shibata R, Ouchi N, Murohara T. Adiponectin and cardiovascular disease. *Circ J.* 2009;73:608–614.
10. Maeda N, Shimomura I, Kishida K, Nishizawa H, Matsuda M, Nagaretani H, Furuyama N, Kondo H, Takahashi M, Arita Y, Komuro R, Ouchi N, Kihara S, Tochino Y, Okutomi K, Horie M, Takeda S, Aoyama T, Funahashi T, Matsuzawa Y. Diet-induced insulin resistance in mice lacking adiponectin/acrp30. *Nat Med.* 2002;8:731–737.
11. Planat-Benard V, Silvestre JS, Cousin B, Andre M, Nibbelink M, Tamarat R, Clergue M, Manneville C, Saillan-Barreau C, Duriez M, Tedgui A, Levy B, Penicaud L, Casteilla L. Plasticity of human adipose lineage cells toward endothelial cells: physiological and therapeutic perspectives. *Circulation.* 2004;109:656–663.
12. Imanishi Y, Saito A, Komoda H, Kitagawa-Sakakida S, Miyagawa S, Kondoh H, Ichikawa H, Sawa Y. Allogenic mesenchymal stem cell transplantation has a therapeutic effect in acute myocardial infarction in rats. *J Mol Cell Cardiol.* 2008;44:662–671.
13. R Development Core Team. R: A language and environment for statistical computing. 2008. R Foundation for Statistical Computing; Vienna, Austria. ISBN 3-900051-07-0. http://www.R-project.org. Accessed August 3, 2011.
14. Kondo K, Shibata R, Unno K, Shimano M, Ishii M, Kito T, Shintani S, Walsh K, Ouchi N, Murohara T. Impact of a single intracoronary administration of adiponectin on myocardial ischemia/reperfusion injury in a pig model. *Circ Cardiovasc Interv.* 2010;3:166–173.
15. Davis ME, Hsieh PC, Grodzinsky AJ, Lee RT. Custom design of the cardiac microenvironment with biomaterials. *Circ Res.* 2005;97:8–15.
16. Yla-Herttuala S, Martin JF. Cardiovascular gene therapy. *Lancet.* 2000;355:213–222.
17. Joung YK, Bae JW, Park KD. Controlled release of heparin-binding growth factors using heparin-containing particulate systems for tissue regeneration. *Expert Opin Drug Deliv.* 2008;5:1173–1184.
18. Allison SD. Analysis of initial burst in PLGA microparticles. *Expert Opin Drug Deliv.* 2008;5:615–628.
19. Xia Z, Triffitt JT. A review on macrophage responses to biomaterials. *Biomed Mater.* 2006;1:R1–R9.
20. Golocheikine A, Tiriveedhi V, Angaswamy N, Benshoff N, Sabarinathan R, Mohanakumar T. Cooperative signaling for angiogenesis and neovascularization by VEGF and HGF following islet transplantation. *Transplantation.* 2010;90:725–731.
21. Hopkins TA, Ouchi N, Shibata R, Walsh K. Adiponectin actions in the cardiovascular system. *Cardiovasc Res.* 2007;74:11–18.
22. Ouchi N, Walsh K. Adiponectin as an anti-inflammatory factor. *Clin Chim Acta.* 2007;380:24–30.
23. Shibata R, Sato K, Pimentel DR, Takemura Y, Kihara S, Ohashi K, Funahashi T, Ouchi N, Walsh K. Adiponectin protects against myocardial ischemia-reperfusion injury through AMPK- and COX-2-dependent mechanisms. *Nat Med.* 2005;11:1096–1103.
24. Shibata R, Ouchi N, Ito M, Kihara S, Shiojima I, Pimentel DR, Kumada M, Sato K, Schiekofer S, Ohashi K, Funahashi T, Colucci WS, Walsh K. Adiponectin-mediated modulation of hypertrophic signals in the heart. *Nat Med.* 2004;10:1384–1389.
25. Tateno K, Minamino T, Toko H, Akazawa H, Shimizu N, Takeda S, Kunieda T, Miyauchi H, Oyama T, Takeda S, Kunieda T, Miyauchi H, Oyama T, Matsuura K, Nishi J-i, Kobayashi Y, Nagai T, Kuwabara Y, Iwakura Y, Nomura F, Saito Y, Komuro I. Critical roles of muscle-secreted angiogenic factors in therapeutic neovascularization. *Circ Res.* 2006;98:1194.